The Life Cycle of Valley Fog. Part II: Fog Microphysics[1]

R. J. PILIÉ, E. J. MACK, W. C. KOCMOND, W. J. EADIE AND C. W. ROGERS

Calspan Corporation, Buffalo, N. Y. 14221

(Manuscript received 29 July 1973, in revised form 8 October 1974)

ABSTRACT

Extensive measurements were made of the microphysics of valley fog in the Chemung River Valley near Elmira, New York. This paper discusses data on drop size distributions, drop concentrations, liquid water contents, and haze and cloud nucleus concentrations obtained on eight fog nights.

The behavior patterns of the microphysical variables were found to be extremely consistent. Shallow ground fog usually occurs prior to the formation of deep valley fog. The data show that ground fog is characterized by droplet concentrations of 100 to 200 per cubic centimeter in the 1 to 10 μm radius range with mean radii of 2 to 4 μm. As deep fog forms aloft, droplet concentration near the surface decreases to less than 2 cm^{-3} and the mean radius increases from 6 to 12 μm. Droplets of radii <3 μm disappear. Thereafter, droplet concentration and liquid water content increase gradually until the first visibility minimum at the surface when typical values range from 12 to 25 cm^{-3} and 50 to 150 mg m^{-3}, respectively. The small droplets reappear at first visibility minimum. Subsequently, bimodal drop size distributions occur in approximately half of the fogs with one mode at 2–3 μm radius and a second mode between 6 and 12 μm. Aloft, drop size distributions become narrower and the mean radius decreases with both increasing altitude and increasing age of the fog. The cloud nucleus concentration active at $S=3.0\%$ is usually between 800 and 1000 cm^{-3} near the surface and decreases to 500–800 cm^{-3} at 300 m.

It is argued from the data that supersaturation in the thin ground fog exceeds that in deep fog. The initial surface obscuration in deep fog appears to be due to droplets that form aloft and are transported downward into unsaturated air by turbulent diffusion. New droplets are apparently not generated near the surface until after the first visibility minimum.

1. Introduction

This paper describes data on the microphysical variables obtained in eight valley fogs which occurred in the Chemung River Valley near Elmira, N. Y., during the summer of 1970. As in Part I, data obtained in the fogs of 22 August 1970 and 2 September 1970 are used to illustrate typical characteristics of fogs that form before and after sunrise, respectively. Data presented here were acquired at the tower site described in Part I.

To our knowledge the data acquired in this investigation constitute the first observations of the evolution of the microphysical properties of fog acquired during the actual formation of the fog, rather than as fog advects over the measurement site. The consistency of the variations of visibility, liquid water content (LWC), drop size distribution, and drop concentration prior to the first visibility minimum near the surface is striking. From some of the consistent changes in the drop size distribution it can be argued convincingly that the degree of supersaturation existing in thin ground fog exceeds that in the deep fog that forms later in the fog life cycle. Furthermore, it appears that the initial visibility degradation near the surface is due to the downward transport of droplets formed aloft and that supersaturated conditions do not exist near the surface until after the first visibility minimum.

[1] This research was conducted under the joint sponsorship of the Aeronautical Vehicle Division of NASA and the Naval Air Systems Command under NASA Contract NASW-2126.

2. Drop size distributions

Measurements of fog drop size distribution were obtained using a modified slide projector to expose gelatin-coated slides to a stream of foggy air. In operation, droplets in the air stream were impacted on the treated slides to leave permanent, well-defined "replicas" that could be accurately measured under a microscope. Previous work had established that true droplet diameter is very nearly equal to one-half the diameter of the crater-like impressions left in the gelatin.

The apparatus was constructed to permit control of exposure time from less than 0.1 s to periods of several minutes and selection of air stream velocity (by a speed control on the blower motor) between 10 and 70 m s^{-1}. To provide for greater accuracy in applying collection efficiency corrections, air velocity was measured for each exposure of the 4 mm wide slides. A similar drop sampler

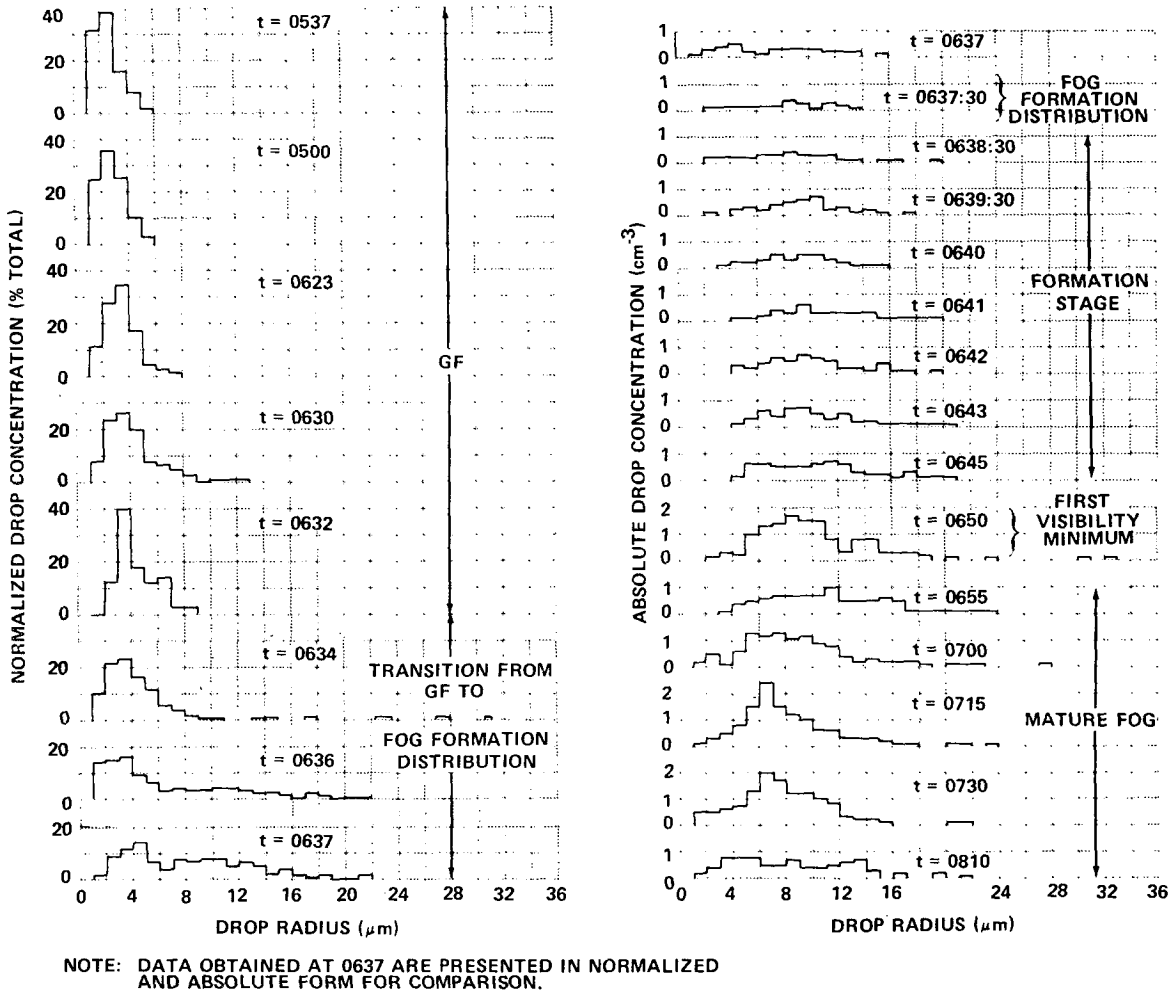

FIG. 1. Drop size distributions for 2 September 1970.

was installed in the nose of a Piper Aztec aircraft to permit collection of drop samples aloft.

Data reduction was performed manually from photomicrographs obtained with a phase contrast microscope. Where possible, a minimum of 200 droplets was measured for each distribution. In some cases of very low droplet concentration, all replicas on the slide were measured directly through the microscope. A total of ~200 surface level (1 m height) drop size distributions from eight fogs was analyzed. A similar number of samples obtained aloft was analyzed.

Inspection of the drop size distribution data obtained at Elmira suggests that droplets $<1\,\mu$m radius could not be detected in the field even though smaller droplets can be detected in the laboratory. The principal known sources of error in these measurements are statistical in nature, imposed by the time required to measure larger numbers of replicas for each distribution. These errors are particularly important for small droplet sizes ($<3\,\mu$m radius) where the number of replicated droplets is limited by small collection efficiencies and, consequently, collection efficiency corrections are large (Langmuir and Blodgett, 1946). Similar problems occur for large drop sizes where natural concentrations are small. A second type of statistical error is due to the lack of "representativeness" of the sample. A fog that occupies several tens of cubic kilometers is often characterized by a few samples, each containing the droplets in volumes from 5 to 10 cm³.

While exposure time for a given sample is controllable, short exposure times ($\lesssim$0.5 s) are not reproducible to within a factor of about 3 from slide to slide. Therefore, normalized drop size distribution data can be obtained directly, but it is not prudent to determine absolute drop concentrations from the droplet samples. Rather, total drop concentrations were obtained by combining the normalized distributions obtained at the surface (1 m) with simultaneous measurements of extinction coefficient obtained from the tower transmissometer (at the 1.2 m height about 30 m away) according to

the expression

$$\beta_{\text{transmissometer}} = 2\pi n \sum_{i=0}^{\infty} N(r_i) r_i^2, \qquad (1)$$

where β is the measured extinction coefficient, n the total drop concentration, and $N(r)$ the normalized drop size distribution.

In many cases in which drop samples were obtained in shallow ground fog, the transmissometer was above the fog top. The visibility within the ground fog was therefore always much less than the transmissometer indicated. The drop size distributions are therefore presented only in normalized form. Data for later periods in the fog life cycle are presented as absolute drop size distributions, given by $nN(r)$.

If measured values for $N(r)$ are used to compute n with typical visibilities measured when ground fog exceeds the transmissometer height, values of n ranging from 100 to 200 cm^{-3} are obtained. These values and the overall size range of droplets observed are in good agreement with previously published data (Jiusto, 1964). Normally, two or three drop samples were taken randomly when ground fog was first observed. When deep fog began to form, samples were usually acquired at intervals of 5–15 min. On 2 September 1970, however, the real-time display of temperature variations with height and time indicated that the formation of deep fog was imminent and a sequence of closely-spaced drop sample collections was initiated before substantial visibility changes were observable. As a result, the most complete data on the evolution of the drop size distribution in valley fog were obtained on that date. The results are presented in Fig. 1.

The drop size distributions obtained prior to 0632 (all times EDT) are characteristic of all distributions obtained in shallow ground fog (i.e., a fairly large number of very small droplets). At 0630 the initial formation of fog was observed aloft, and drop sampling was started at 2 min intervals. Seven minutes later the first decrease in surface visibility was noted, and the sampling interval was shortened to 1 min or 30 s when possible.

The distribution obtained at 0637:30 is characteristic of the distributions obtained at the time of the initial surface visibility decrease on all fog days. Data obtained between 0634 and 0637 show the transition from characteristic ground fog distributions to what we have named the "fog formation distribution." On this date, the fog formation distribution persisted for only a few minutes. On one occasion, 26 August 1970, however, that distribution persisted for 45 min before dense fog formed.

Data obtained between 0638:30 and 0650 illustrate the characteristic changes in drop size distribution that occur between the initial visibility decrease and the first visibility minimum. These changes include 1) the

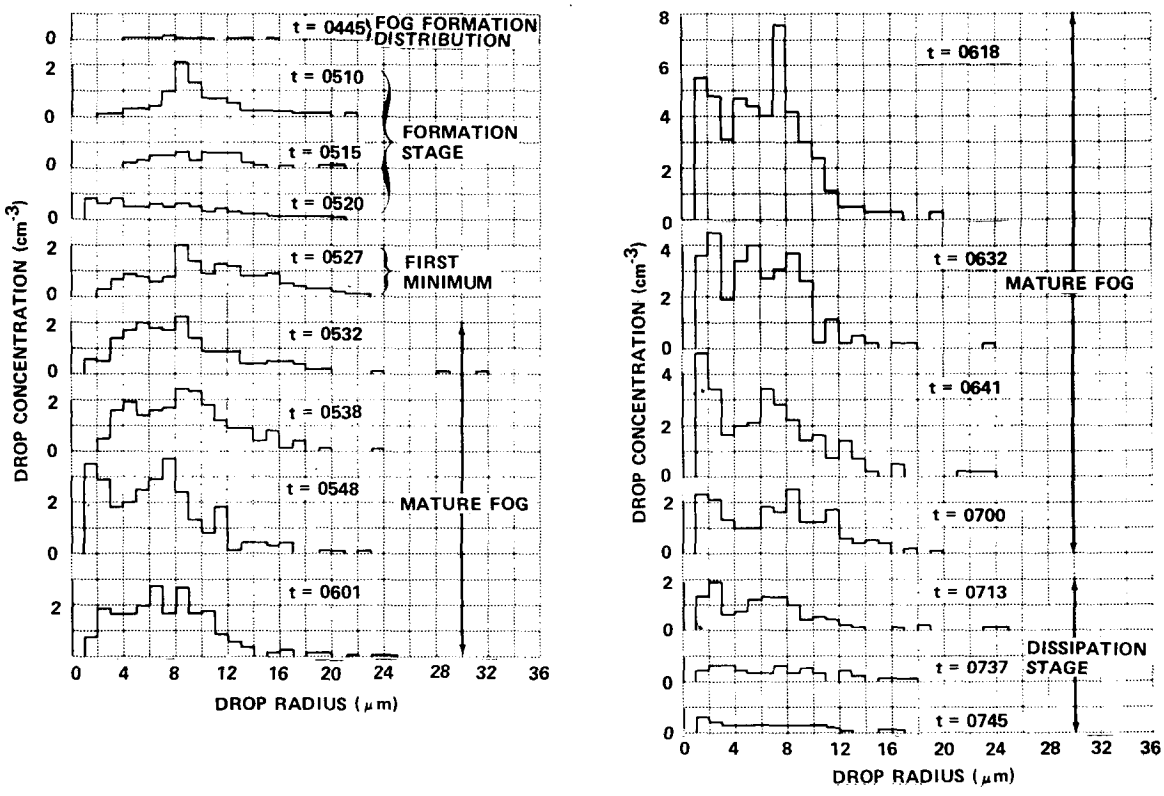

FIG. 2. Drop size distributions for 25 August 1970.

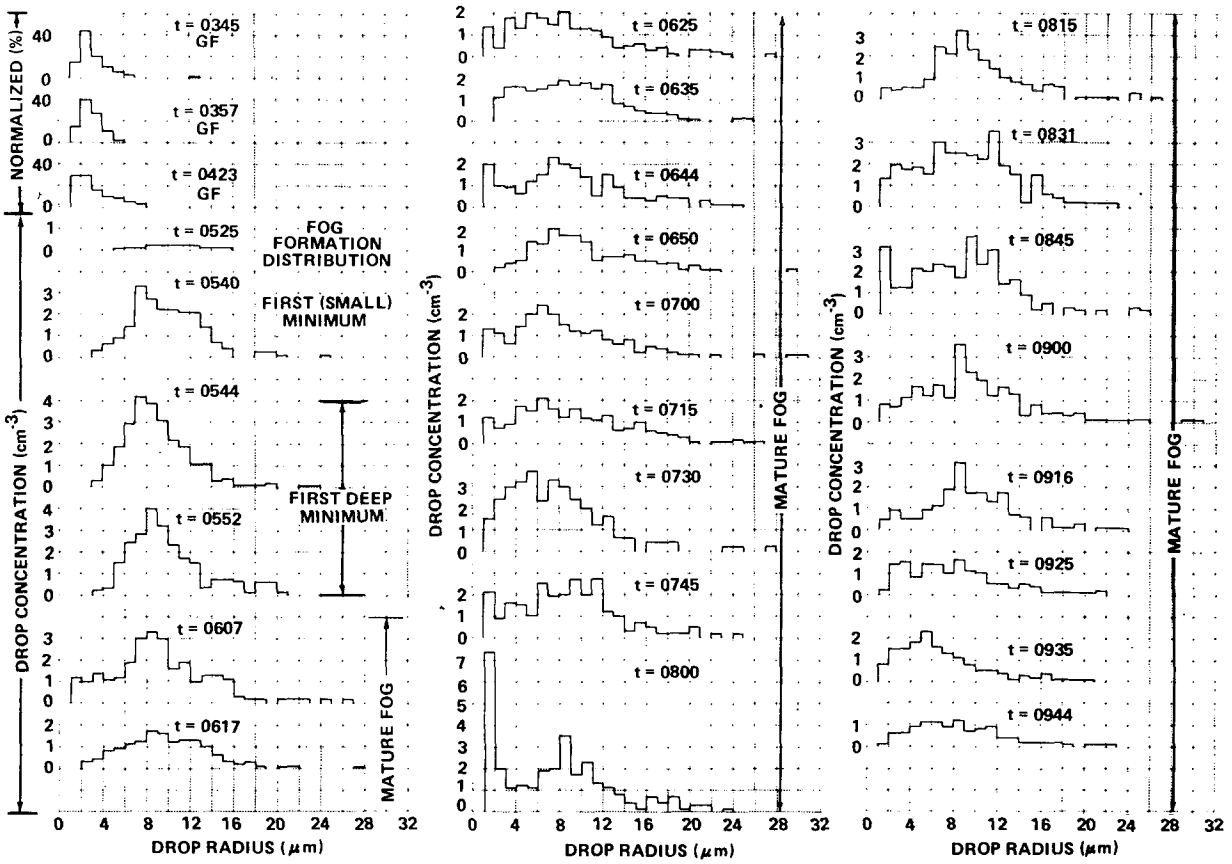

FIG. 3. Drop size distributions for 22 August 1970.

disappearance of droplets smaller than 3 or 4 μm radius, 2) a gradual increase in drop concentration to maximum, and 3) an increase in the maximum drop size to the largest values observed throughout the fog life cycle.

The very small droplets consistently reappear shortly after the first visibility minimum. From that time on, however, the behavior of the drop size distribution with time is not completely consistent. In three of the eight fogs sampled, all distributions obtained at the surface after the first minimum were similar to those shown for 2 September 1970 between 0700 and 0810. On three other occasions, surface drop size distributions obtained after the first minimum were predominantly bimodal, with a maximum near 2–3 μm radius and a second maximum between 6 and 12 μm. Typical distributions of this kind are illustrated in Fig. 2 (for times after 0538). On two occasions, distributions of both kinds seemed to occur randomly through the fog life cycle as illustrated in Fig. 3. No consistent change in the shape of the surface drop size distribution associated with fog dissipation was apparent. The concentration of droplets in each size interval simply decreased as visibility improved.

3. Liquid water content

Data on liquid water content (LWC) were acquired by integrating the absolute drop size distribution

$$\omega = (4/3)\pi n \sum_{i=0}^{\infty} N(r_i) r_i^3$$

for each drop sample and occasionally (5 to 10 times per fog) by direct measurement using a Gelman[2] high-volume sampler for mechanical collection of the water from 8 m^3 of fog. Cellulose filters were used in the Gelman so that liquid water was absorbed into the fibers. To minimize the error due to the absorption of water vapor from the humid atmosphere by the cellulose, the filters were moistened by the collection of water from 2 m^3 of fog prior to the first weight measurment. The increase in weight after exposure to an additional 8 m^3 of fog was used to determine LWC. Simultaneous measurements of LWC by the two methods are compared in Fig. 4. In general, the two procedures exhibit agreement to within ± 40 mg m^{-3}. Variability appears to be random and is undoubtedly associated in part with the fact that Gelman data were

[2] Gelman Model No. 16003.

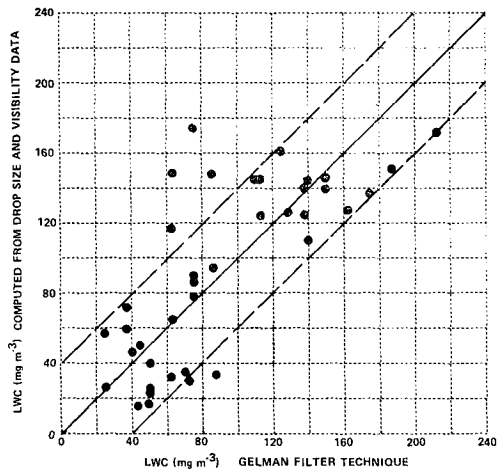

FIG. 4. Comparison of liquid water content measurements made with a Gelman high-volume sampler and simultaneous values obtained by integrating the absolute drop size distributions.

obtained from an average of 8 m³ of fog acquired over a 7 min interval while the drop-size distributions were acquired from a few cubic centimeters of fog collected essentially instantaneously.

SUMMARY OF FOG MICROPHYSICS AT THE SURFACE

Time histories of fog microphysics at the surface, including drop concentration, liquid water content and mean, mean-squared and mean-volume droplet radii with time are presented for the two sample fogs in Figs. 5 and 6. The tower site visibility trace is also presented on each figure. [Note that in Fig. 5 (2 September 1970) the time scale has been expanded.]

Since the principal variations in fog microphysics at the surface occurred during the first and last quarters of the fog life cycle, regardless of total fog duration, an attempt was also made to model the microphysics data on a time scale defined by fractions of total fog duration. Averages of all available data from seven fogs were computed for each phase of the respective life cycle. The data are summarized in Fig. 7. The onset of fog was arbitrarily set as the time when visibility degraded to <4000 m; a visibility increase to 1000 m was chosen as the end of fog. As indicated by the data, visibility usually degraded rapidly from 4000 m to a minimum value and improved somewhat more slowly to 1000 m as fog "lifted" near the end of its life cycle.

These figures taken together illustrate the pertinent microphysical characteristics observed throughout the life cycle of most Elmira valley fogs, which can be summarized as follows:

1) Visibility degrades to a minimum during the first quarter of the life cycle and then slowly improves. Through the middle half of the life cycle (the mature fog), visibility may remain nearly constant or undergo large fluctuations. The dissipation stage accounts for the last quarter of the life cycle.

2) Droplet concentration and liquid water content increase to a maximum at the time of the first visibility minimum, fluctuate synchronously with visibility during the mature stage, and decrease drastically during the dissipation stage.

3) The mean, mean-square and mean-volume radii of the drop size distributions increase to near maximum approximately midway between the first observable visibility decrease and the first visibility minimum. The mean sizes then gradually decrease and maintain near-constant values through the mature stage. While the average data indicate a decrease in mean radius at the time of dissipation, data from individual fogs show no consistent changes in *mean* drop size associated with the dissipation stages.

4. Drop size distributions aloft

Because of flight restrictions limiting takeoffs under dense fog conditions prior to daylight hours, drop size distribution data aloft could not be obtained before the

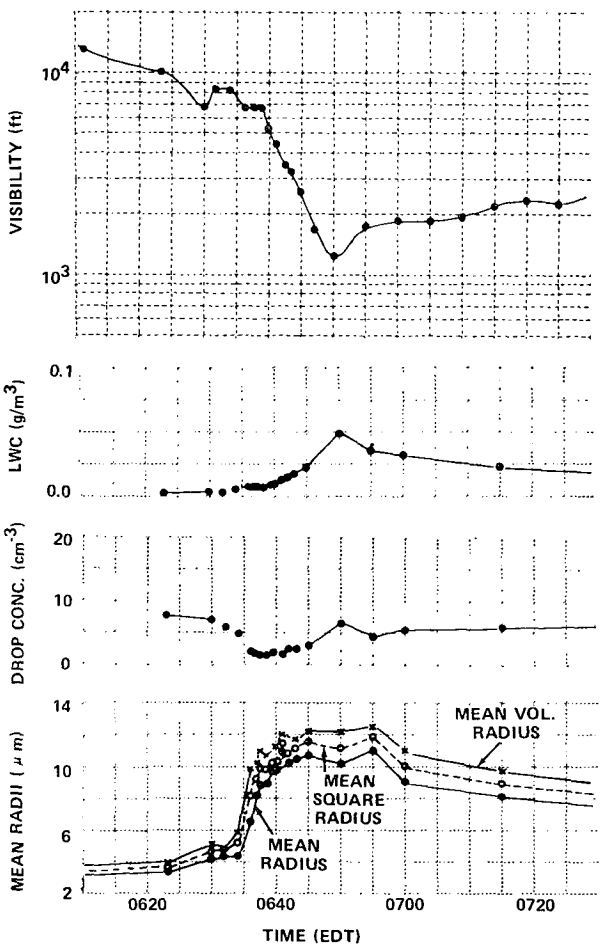

FIG. 5. Visibility and microphysics data for 2 September 1970.

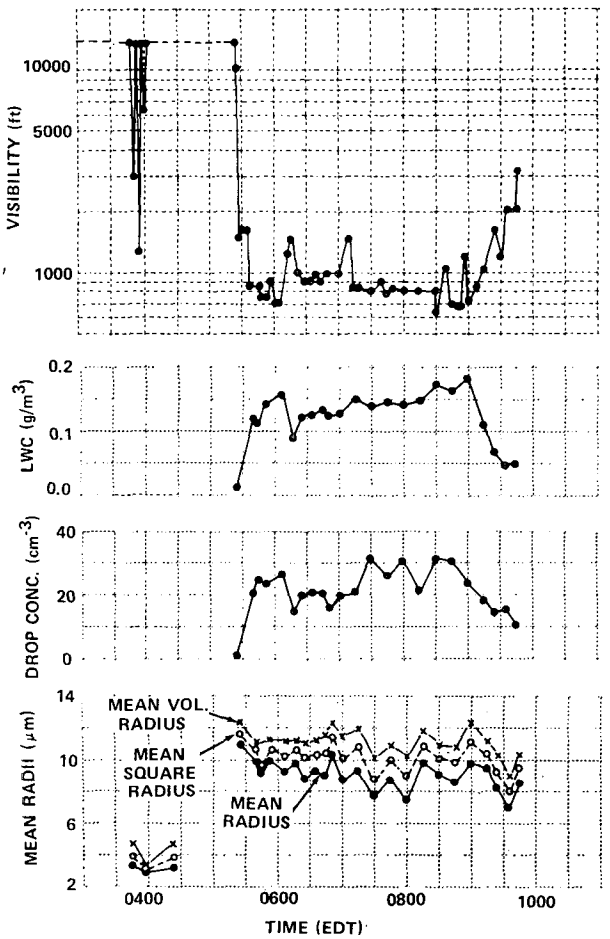

FIG. 6. Visibility and microphysics data for 22 August 1970.

first visibility minimum. The data acquired after daybreak, however, display consistent behavior with both height and time. This behavior is illustrated by the data acquired on 22 August 1970 and 12 September 1970 presented in Figs. 8 and 9.

Since there are no visibility data aloft, all distributions are presented in normalized form. Note from the figures that the broadest drop size distributions were observed at or near the surface at all post-daybreak times during the fog. During the earliest sounding, the drop spectra always exhibited only a slight decrease in width of the distribution with altitude, but as time progressed, the distributions aloft became more and more peaked in the small size range. Exceptions occurred at low levels near the end of the dissipation stage when fog lifted off the surface and visibility exceeded one-half mile. Distributions aloft that were more typical of surface distributions were occasionally obtained under these conditions.

The general trend toward smaller drops aloft with increasing altitude and time is best illustrated by the vertical profiles of mean radius for successive soundings. That format is used in Fig. 10 to present data acquired during four fogs that are representative of all fog types sampled (22 August and 12 September 1970, persistent fogs; 13 August 1970, patchy fogs; 2 September 1971, short fogs that form after sunrise). Mean droplet radius data from all fogs were averaged to provide a model of the droplet profile for valley fog at Elmira. The data are presented in Fig. 11 and are summarized according to fractions of the fog life cycle (as in Fig. 7) and normalized to fractions of fog depth (typically 120 m). The decrease in mean radius with height and time is clearly evident from the data. The data further show that in the early stage of the fogs mean drop size was relatively constant with altitude, but that later drop size decreased substantially with height probably due to the combined effects of droplet settling and evaporation of the smallest drops near the surface after sunrise.

5. Cloud nucleus observations

The aircraft was used to obtain measurements of cloud condensation nuclei (CCN) at several selected altitudes prior to fog formation. Observations of CCN at 0.3%S were made at the surface and at altitudes of 30, 90, 150 and 300 m. Flights normally were scheduled at midnight, 0300 and also 0600 EDT if fog had not already formed.

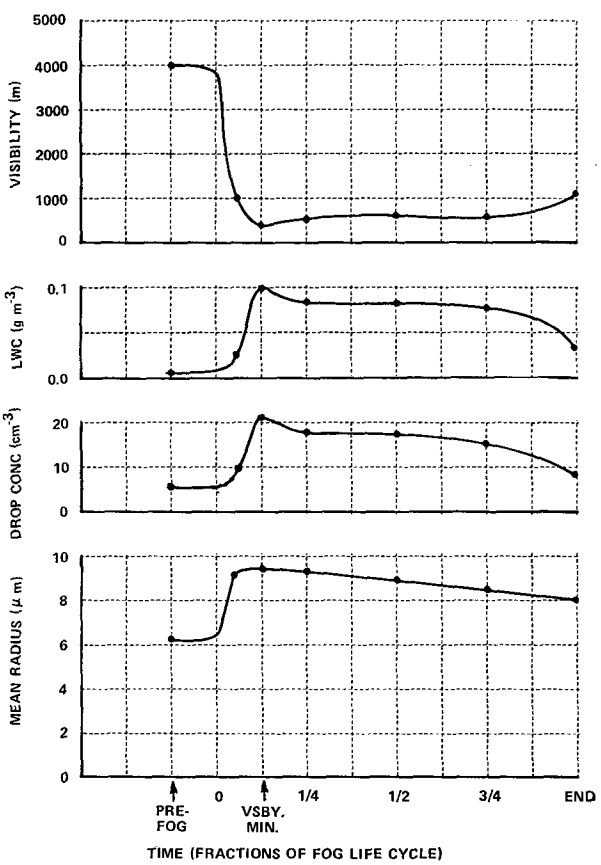

FIG. 7. Average fog microphysics as a function of its life cycle.

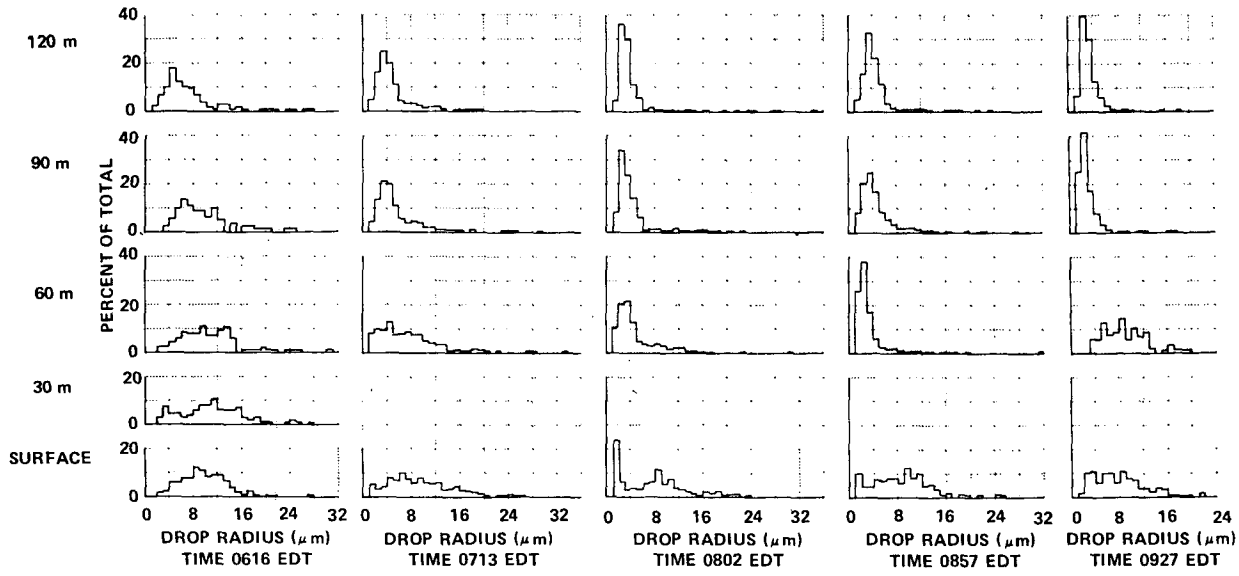

FIG. 8. Normalized drop size distributions aloft for 22 August 1970.

In Fig. 12, average CCN data are shown for the three flight times. Data obtained on 12 flights were used in tabulating the averages at 0000 and 0300, but fewer flights were possible at 0600 because of some early occurrences of fog. The data show that CCN concentrations are greatest near the ground and generally decrease with altitude in the valley. It is of some interest to note the abundance of cloud nuclei that are present even in the relatively clean rural environment near Elmira. By comparison, measurements of average CCN in the vicinity of the more highly industrialized area of Buffalo over a three-year period were nearly the same or about 1000 cm^{-3} at 0.3%S (Kocmond and Jiusto, 1968). No large differences in the CCN concentrations were found between nights with and without fog. Since the population of fog drops is always much smaller than the population of nuclei activated at 0.3%S, this result is not surprising. No attempt was made to measure CCN in fog since there is reason to doubt the accuracy of such observations at high relative humidities (Saxena *et al.*, 1970; Fitzgerald, 1970).

Possibly a more sensitive indicator of variations in

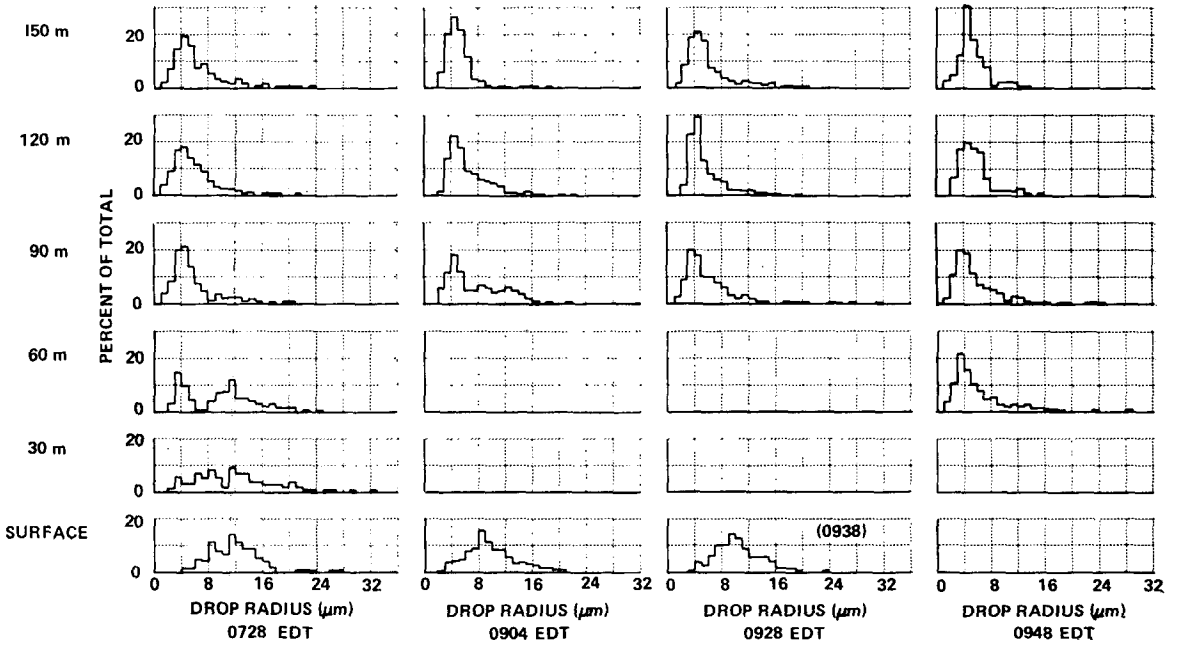

FIG. 9. Normalized drop size distributions aloft for 12 September 1970.

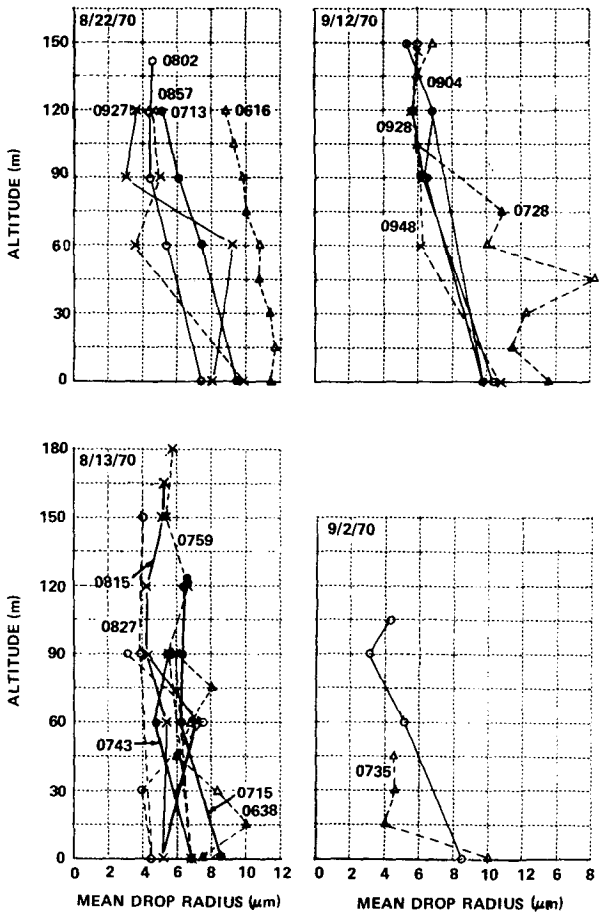

FIG. 10. Variations of mean drop radius with time and height.

the spectrum of "large" and "giant" nuclei that participate in fog formation can be found from the use of the haze chamber. This device, which received only limited use on the program, is similar in most respects

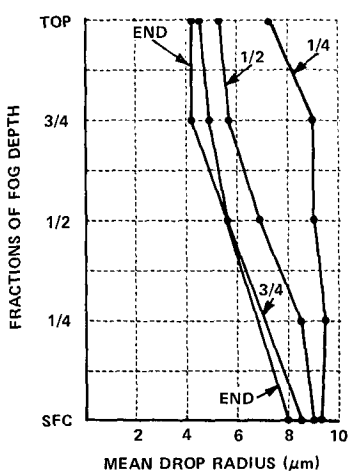

FIG. 11. Average vertical profiles of mean drop radius at fractions of the fog life cycle.

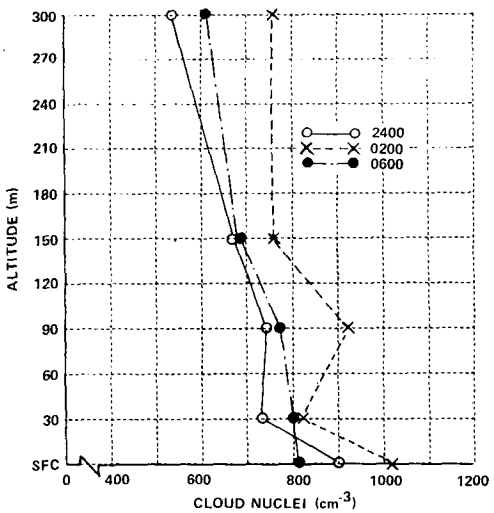

FIG. 12. Vertical profiles of cloud nucleus concentration at three times using average data from 12 flights at $S=0.3\%$.

to the thermal diffusion cloud chamber, the only difference being that saturated solutions of KNO_3 are used in place of the upper and lower water reservoirs. It is possible, therefore, to produce controlled relative humidities in the range 95% to 100%, thereby activating (i.e., enlarging r to 1 μm or greater) only the largest and most favorable cloud nuclei.

The data in Fig. 13 show results of observations of haze and cloud nuclei on 10 and 12 September 1970. The wide differences in haze nucleus concentration on these two dates are particularly noteworthy, especially since the CCN count at 0.3%S was nearly the same on both days. There was no fog on 10 September. On 12 September ground fog formed at about 0350 and wide-

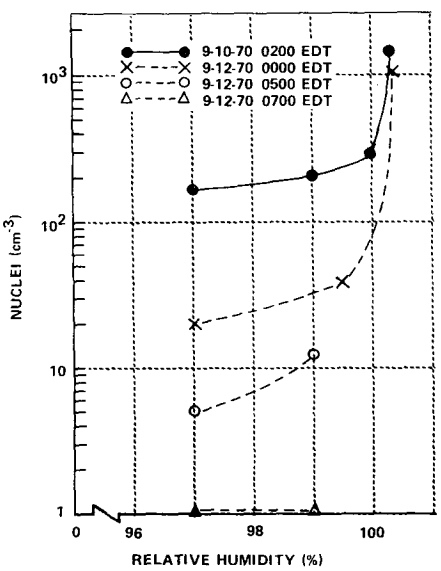

FIG. 13. Haze nuclei data,

spread dense fog developed by 0500. Prior to fog formation, the haze concentration at 99% RH was about 40 cm^{-3}; later, after fog had developed, the count fell to less than 10 cm^{-3}. Still later in the period, after fog had persisted for several hours, no haze nuclei at all were observed in the chamber. These data suggest to us that many of the haze nuclei observed earlier in the day contributed to the formation and persistence of droplets in the dense fog that developed at the airport. Unfortunately, no additional observations were made after fog dissipation. In future field programs, it is suggested that the haze nucleus concentration be examined prior to, during and after fog formation. In this way it may be possible to measure the concentration of those nuclei that actually produce fog droplets.

6. Discussion and summary

The data presented in Figs. 1 and 3 show that the drop size distributions that exist prior to formation of deep fog are consistently characterized by a mode between 2 and 4 μm radius and a maximum of about 8 μm. Between 65% and 95% of the droplets in each distribution have radii $>2\,\mu$m, suggesting that the observed droplets were not simply enlarged nuclei, i.e., the nuclei were fully activated to droplet growth. As indicated in the data presentation, these droplets characterize the ground fog which was usually below the level of the transmissometer. For this reason, absolute concentration cannot be established. Calculations based on transmissometer data obtained when the beam passed through the ground fog indicate typical droplet concentrations of 100–200 cm^{-3}.

Through the early morning hours, ground fog was often observed to dissipate and reform. From the data presented in Figs. 1 and 5 for the fog of 2 September, it appears that the ground fog droplets persisted until deep fog formation but that drop concentration decreased before deep fog formed.

Changes in drop concentration may be due to a combination of the low-level warming that precedes fog formation and to the vertical mixing that increases significantly during the period of deep fog formation. (See Part I of this paper.) In any case, it is apparent that the supersaturation present in the ground fog is sufficient to support the presence of 60–200 droplets cm^{-3} and therefore to produce full activation of those concentrations of cloud nuclei. These concentrations are greater by a factor of 2 to 10 than droplet concentrations observed in the deep fog. If it is assumed that the activation spectrum of the nuclei in the region in which ground fog forms is the same as at high altitudes in the valley, which appears reasonable from the data, it follows that supersaturation at the time of formation of ground fog is significantly greater than during formation of the deep fog.

This conclusion seems acceptable upon consideration of the temperature distribution through the two fog depths. The mean temperature difference is approximately 2.5°C between the 1 and 0.1 m levels during the 6 h before deep fog formation. If equal air parcels from each of these levels are mixed, the supersaturation developed (before vapor depletion by droplet growth) would be ~0.3%. Without vapor depletion, the cloud nuclei data (Fig. 12) indicate that ~1000 nuclei cm^{-3} would be activated. With the existing vapor losses, the supersaturation attained is less and apparently just sufficient to produce 100–200 droplets cm^{-3}.

The data presented in Fig. 10 of Part I indicate a maximum temperature difference of about 1°C over a 100 m depth during the interval in which deep fog forms. Mixing of two saturated air parcels at the temperature extremes would produce a supersaturation slightly exceeding 0.1% if such mixing could occur. Considering the extreme separation of these air parcels, it is obviously impossible for such mixing to occur without thorough dilution by air from other levels.

While the supersaturation at the time of ground fog formation exceeds that for deep fog, the drop size distribution in ground fog remains narrow throughout its life cycle. This is partially due to precipitation of the largest drops (e.g., a droplet of 5 μm radius falls through the 1 m depth in ~5 min) and is also associated with vapor depletion by the high concentration of existing droplets. Available water must be distributed over a higher concentration of nuclei so that no one droplet can grow rapidly. For obvious reasons, these mechanisms are not as effective in deep fog and the equilibrium drop size distribution is significantly wider.

The consistent pattern in the evolution of the drop size distribution between the fog formation distribution and the first visibility minimum is intriguing. The fact that droplets with radii <3–$4\,\mu$m were, with one exception, never detected during this period in which the total concentration of droplets was increasing deserves explanation. There appears to be an internal conflict in the data, i.e., large droplets seem to form without going through the small droplet stage.

One hypothesis which was considered in attempting to explain these observations is that the time required for growth of a new droplet from its critical radius (i.e., its radius at the maximum of the relevant Kohler curve) to 3 μm radius is so short and the concentration of drops in the 1–3 μm size range at any time is so small that the probability of detection of one of these droplets with our sampling procedure is essentially zero.

Excluding the fog of 15 August 1970, the average maximum rate of increase in drop concentration was 0.6 cm^{-3} min^{-1}. On 15 August 1970, the only case in which small drops were observed during the formation stage of deep fog, the rate was 2.6 drops cm^{-3} min^{-1}. Since droplets $<3\,\mu$m radius are seldom observed, the hypothesis stipulates that the average concentration of droplets in this range must be smaller than 0.1 cm^{-3}, which is the minimum concentration that is consistently

detected with our sampling procedures. If we consider the average concentration to be a time average, it is necessary that the fraction of any long-time interval during which a given cubic centimeter of air is occupied by at least one droplet smaller than 3 μm radius is substantially less than 0.1. Otherwise, droplets in this size range would be detected. This fraction of the time is given by the product of the production rate of droplets and the time τ required for a newly activated droplet to grow to 3 μm radius. To go undetected, therefore:

$$\left.\begin{aligned} &0.1 < 0.6 \text{ cm}^{-3} \text{ min}^{-1} \times \tau \text{ min} \\ &\tau < 0.17 \text{ min} = 10 \text{ s} \end{aligned}\right\}.$$

We may now ask whether or not the supersaturation required to produce such rapid growth can exist near the surface during fog formation. Using the approximate droplet growth equation given by Fletcher (1966), computations were made of the growth at 0.3%S of drops that form on nuclei with different activation thresholds. The results are presented in Table 1.

It is obvious from these values that the time required for droplet growth on nuclei with even significantly lower activation thresholds than the existing supersaturation substantially exceeds the 10 s limit established above. Even larger supersaturation would therefore be required to explain the observations on the basis of this hypothesis. Since the data presented in Fig. 12 show that the concentration of nuclei activated at 0.3% S is of the order of 800 cm^{-3}, we know that such supersaturations do not exist in the region of the measurement.

It must be concluded from this analysis that the increase in concentration of droplets near the surface during deep fog formation is not due to activation of new nuclei in the region where the observations were made.

It is conceivable under some fog conditions that sporadic supersaturations exceeding 0.3% could be produced in small regions by mixing of two near-saturated air parcels with different initial temperatures. The required temperature differences exceed those which were observed within the fog however. Since the response time of our temperature sensors is of the order of 0.5 min, it is possible, but not likely, that small patches of cool and warm air did exist simultaneously in the region of fog formation.

A more realistic hypothesis for explaining the increase in droplet concentration at the surface during the fog formation stage is that the droplets are transported to the surface by turbulent diffusion from aloft. Under this assumption, the initial appearance of deep fog at the surface could occur during a period in which the surface atmosphere is slightly subsaturated. With the fog existing aloft for times ranging from one-quarter to one hour before the first decrease in surface visibility, it is not necessary to postulate such rapid droplet growth and high supersaturations in order to cause most of the droplets to grow to radii >3 μm. The generation of new droplets can proceed continuously at higher altitudes. Upon being trapped in turbulent eddies, the droplets are carried downward. The associated warming promotes evaporation which tends to produce a wet adiabatic lapse. With the driving function for evaporation under a moist adiabatic lapse being a 0.02% supersaturation reduction per meter of descent, evaporation of newly formed small droplets can begin even before the eddy reaches the existing fog base.

TABLE 1. Growth of droplets at 0.3%S on nuclei of different activation supersaturations.

Radius of dry NaCl particle (μm)	Activation threshold (% S)	Droplet size (μm) at indicated time		
		5 s	10 s	20 s
0.020	0.45	0.12	0.13	0.14
0.025	0.32	0.20	0.20	0.20
0.032	0.23	1.17	1.85	2.82
0.040	0.16	1.33	1.95	2.90

If this level is 20 m, for example, evaporation may proceed for periods exceeding 100 s at the typical downward velocities observed on 12 September 1970 (Fig. 15, Part I) during the fog formation period. With the lower atmosphere already slightly subsaturated, the extremely small droplets can disappear.

The reappearance of small droplets during the first visibility minimum appears to signal the onset of supersaturated conditions near the surface, or at least of conditions that are so close to saturation that evaporation of even the small droplets proceeds slowly. The presence of high concentrations of droplets of 2–3 μm radius observed in some fogs is consistent with activation of new nuclei into droplet growth and the subsequent slow growth that would be expected at low (e.g., less than 0.1%) supersaturation.

In summary, detailed analysis of valley fog microphysics data lend additional support to conclusions presented in Part I of this paper. The data clearly indicate that while shallow ground fog may on occasion exist prior to formation of deep valley fog, the formation of deep fog occurs first aloft due primarily to cooling at that level brought about by nocturnal valley circulations. Further radiative cooling at fog top produces an unstable lapse within the fog which must eventually extend below fog base. Continued cooling and subsequent turbulent transport cause the fog base to propagate downward to the surface; evaporation of the smallest droplets below fog base gives rise to the initial observations of large drops in dense valley fog.

After sunrise, dissipation begins throughout the entire fog layer (evidenced by the vertical profiles of mean drop size) but is somewhat retarded because of evaporation of dew. Once dew evaporation can no longer maintain saturation, fog dissipates at the surface and the fog "lifts."

REFERENCES

Fitzgerald, J. W., 1970: Non-steady-state supersaturations in thermal diffusion chambers. *J. Atmos. Sci.*, **27**, 70–72.

Fletcher, N. H., 1966: *The Physics of Rainclouds*. Cambridge University Press, 390 pp.

Houghton, H. G., and W. R. Chalker, 1949: The scattering cross section of water drops in air for visible light. *J. Opt. Soc. Amer.*, **39**, 955–957.

Jiusto, J. E., 1964: Investigation of warm fog properties and fog modification concepts. NASA, CR-72.

Kocmond, W. C., and J. E. Jiusto, 1968: Investigation of warm fog properties and fog modification concepts. NASA, CR-1071.

Langmuir, I., and K. Blodgett, 1946: A mathematical investigation of water droplet trajectories. USAF Tech. Rept. No. 541B.

Saxena, V. K., J. N. Burford and J. L. Kassner, Jr., 1970: Operation of a thermal diffusion chamber for measurements on cloud condensation nuclei. *J. Atmos. Sci.*, **27**, 73–80.